INFLUENCE OF HEAT TREATMENTS ON MICROSTRUCTURE, MECHANICAL

PROPERTIES AND CORROSION BEHAVIOUR OF ALLOY 625 FORGED ROD

Chantal Vernot-Loier , François Cortial

DCN Indret, Laboratoire d'Etudes et de Contrôle des Matériaux 44 620 La Montagne, FRANCE

Abstract

Influence of heat treatments between 500 and 1125°C on forged alloy 625 has been studied. Hardening between 650 and 800°C results of dislocation glidings of matrix, χ'' precipitation and maximum of intergranular precipitation of fine M23C6 carbides. Tensile strength and intergranular corrosion through ASTM G 28 test become maxima, impact strength and reduction of area become minima, in the field of M23C6 and M6C intergranular precipitation: between 700 and 950°C.

Introduction

Nickel alloy 625, typically containing 22 wt.% Cr, 9 wt.% Mo, 3,7 wt.% Nb and < 5 wt.% Fe , combine good mechanical properties, weldability and corrosion resistance (1). It has numerous applications in chemistry, pulp and paper (2), offshore and marine industries (3), and in geothermal power systems (4).

Alloy 625 is an interesting alloy for our applications, because it may be used to join by welding dissimilar metals such as low alloy steels, High Strength Low Alloy steels with alloy 625, to repair these steels by welding (5-7) or to clad them to protect against corrosion (8-10). In such cases, post-welding heat treatments may be necessary to keep good properties in the heat affected zone of the ferritic steels. But there are few results (11-13) on the influence of heat treatments on the structure and properties of alloy 625.

The stiffening effect of molybdenum and niobium on the nickel-chromium matrix is responsible for strength and two types of solution treatments could be chosen:

- between 930 and 1040°C to improve tensile strength and corrosion resistance,
- between 1090 and 1200°C to improve creep resistance.

Intermetallic compounds and different sorts of carbides are able to precipitate in the face centered cubic matrix and in the grain and twin boundaries during further heat treatments. Thus, a precise study of heat treatments between 500 and $1125\,^{\circ}\text{C}$ is necessary.

The purpose of the work reported in this paper was to determine the relationship between heat treatments, structure, mechanical properties and corrosion resistance.

Tests

Material

A 150 mm \times 20 mm forged rod was purchased. The alloy was vacuum remelted. Table I shows the chemical composition of the rod.

Table I Chemical composition of as-received forged rod

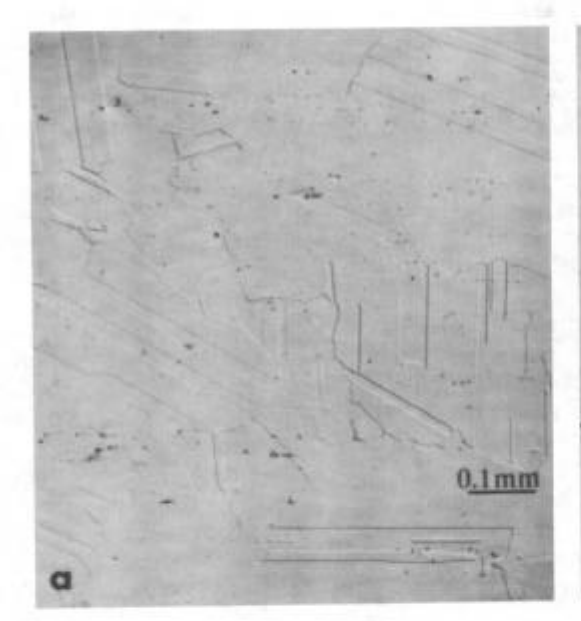
Elements	С	Si	P	S	Al	Тi	Fe	Nb	Co	Çr	Мо	Mn	Ni
wt %	0,019	0,15	0,008	0,001	0,2	0,26	3,7	3,4	0,1	21,4	8,7	0,07	61,8

Table II shows the mechanical properties of the as-received material and after 1 h at 1125°C, then water-quenched. The structure obtained after this treatment is given in figure 1, with inclusions of carbides and carbonitrides of Nb and Ti and oxides inside the fcc twinned grains. This high

temperature solution treatment was chosen to study a heat state similar of those of welded alloy 625 but with a chemical composition as homogeneous as possible, to avoid artefacts due to segregations. This is the reference state for our study.

Table II Mechanical characteristics of as-received rod and material solution-treated 1 h at 1125°C and waterquenched

Characteristics	0.2 % YS (MPa)	UTS (MPa)	EL (%)	RA (%)	CVN energy
	607	1012	41	58,8	160 160
As-received	588	1011	34	57	165
solution-treated	336	768	61	71	295
1 h - 1125°C and water-quenched	332	767	61	71	295 285



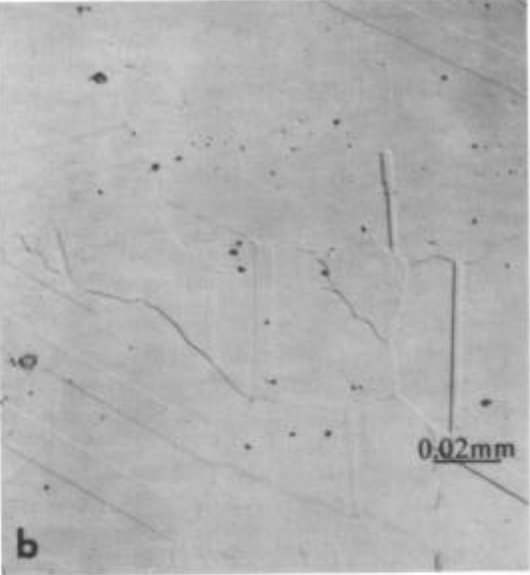


Figure 1 - Optical micrographs of sample solution-treated 1 h at 1125°C and water-quenched.

- a) general view -
- b) detail view.

Heat treatments

160 mm length pieces of rod were heat treated 8 h at temperatures spaced of 50°C between 500 and 1050°C , and also at 1125°C , with heating rate of 50°C/h and air cooling.

Sampling is shown in figure 2.

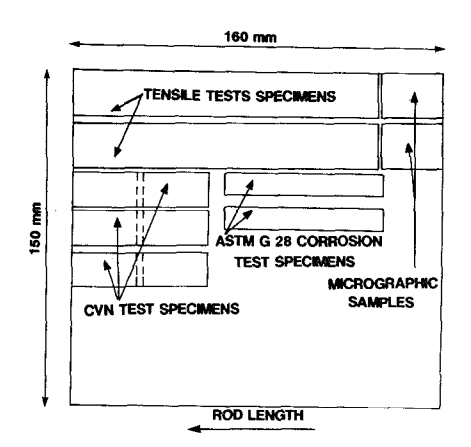


Figure 2 - Sampling.

Structural investigations

Optical microscopy . All the heat treated samples were examined by optical microscopy using natural light and Interferential Differential Contrast (IDC) techniques , which enhances morphological and topographical phases differences. The micrographic samples were mechanically polished with alumina, and then electrolytically etched in a bath containing chromic anhydrid 25g, acetic acid (d=1,05) 130 ml, distilled water 7 ml, with power supply: 7 V d.c., during 1 to 2 min. depending on heating state.

Scanning Electron Microscopy (SEM). Before and after corrosion tests, samples were examined by means of SEM JEOL 840 equipped with an inclined Energy-Dispersive X-ray Spectrometer (X-EDS) EDAX ECON 9100.

Scanning Transmisson Electron Microscopy (STEM). The microstructural study of the heat treated samples has been performed with a STEM JEOL 2000 FX equipped with a horizontal X-EDS microzhv TRACOR Northern. Cristallographic calculations were done with the EDPA program of TRACOR Northern. Bright Field (BF), Dark Field (DF), and Selected Area Diffraction (SAD) techniques have been used. Thin foils for STEM were cut with a coated diamond wire-saw, down to 0.1 mm thickness and then thinned in a twin-jet electropolisher under different conditions depending on heat treatment state (Table III).

Table III Twin-jet electropolishing conditions for thin foils.

Heat treatments	Bath	Temp.	I (mA)	V (v)	Time (s)
500°C to 750°C	95 % acetic acid + 5 % perchloric acid	+3-+15	40 -> 200	40→ 60	20 120
800°C to 1125°C	90 % ethanol + 10 % perchloric acid	0-+3	100→500	15 -> 50	20-> 70

Mechanical properties.

The same tests were performed after each heat treatment.

Hardness tests. The Vickers hardness was measured using 10 kgf and 30 kgf load, on microscopically polished samples.

Tensile tests. The Yield Strength (YS 0.2 % offset), the Ultimate Tensile Strength (UTS), the Elongation (EL) and the Reduction of Area (RA) were determined at room-temperature, on two specimens which gage length equals five diameters, and taken with their great axis parallel to the rod length.

CHARPY Impact strength test. CHARPY Impact strength test has been performed at room-temperature, on three V-notch specimens taken with their great axis parallel to the rod length.

After test, fracture surfaces were examined in SEM.

Intergranular corrosion test

ASTM G 28 intergranular corrosion tests were performed on two samples of 70 mm x 10 mm x 3 mm for each heat treatment, with their great axis parallel to the rod length. ASTM G 28 test conditions were strictly applied except for two points :

- one of the large side of each sample was mechanically polished with 6 μ m diamond, to make possible microscopical investigations after tests. The other sides were polished under water with P 120 paper.
- some tests concerning the most sensitive samples were shortened to be able to examine the beginning of the attack and to avoid a Fe^{3+} depletion in the solution: 6 to 70 h compared to 120 h for normal test time.

After test, the weight losses of samples were converted into corrosion rate in mm/year and corrosion features were observed in SEM.

Results

Structural changes

Structural changes are summarized in figure 3.

Up to 650°C, no structural difference exists between reference state (1h at 1125°C, water-quenched) and heat treated samples.

From $650\,^\circ\text{C}$ above, a rare linear network appears in some \ref{N} matrix grains with an approximate angle of 70 degrees, between the directions. This phenomenon increases and becomes general at $700\text{-}750\,^\circ\text{C}$ (Fig.4a). No precipitation has been observed in STEM for the sample heat treated at $650\,^\circ\text{C}$. Only dislocation arrays along the {111} matrix planes corresponding to dislocation glidings take place (Fig.4b).

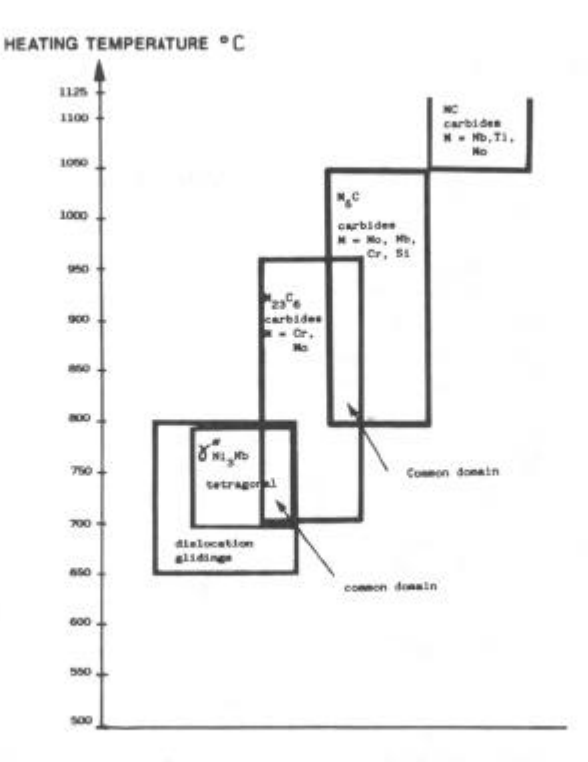
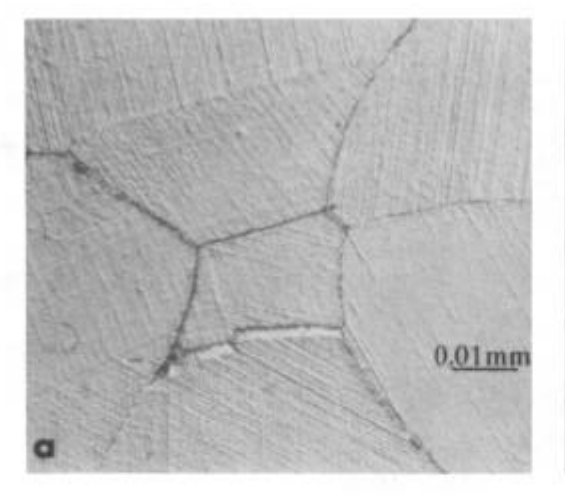


Figure 3 - Phases stability of Inconel 625 heat treated.



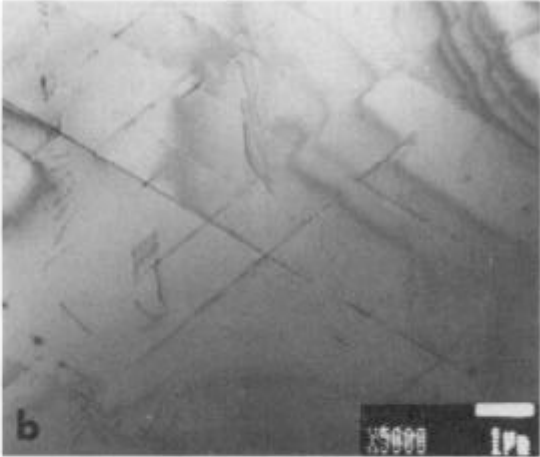
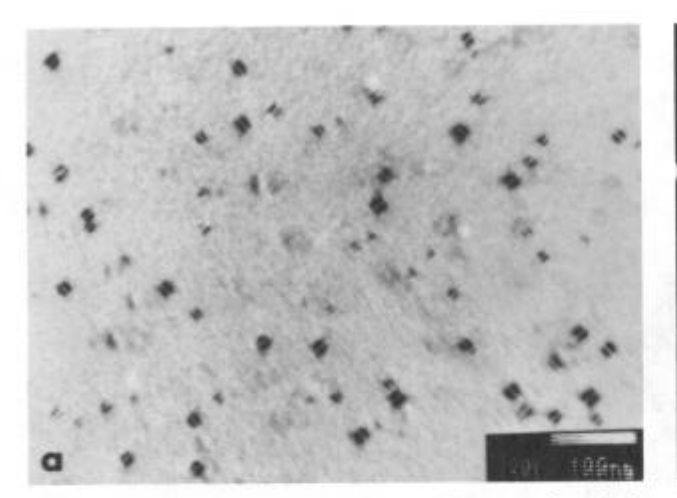


Figure 4 - Optical and TEM micrographs of dislocation glidings of matrix.

- a) optical microscopy -
- b) transmission electron microscopy.

From 700°C above, this phenomenon increases and the % matrix present a speckled appearance due to the precipitation of the coherent intermetallic phase % " Ni₃Nb tetragonal (Fig.5). At the same temperature, M₂₃C₆ (M = Cr, Mo) fine carbides (<200 nm) precipitate at matrix grain boundaries (Fig.6). They are nucleated separately on both sides of grain boundaries with coherent boundary on its matrix side.



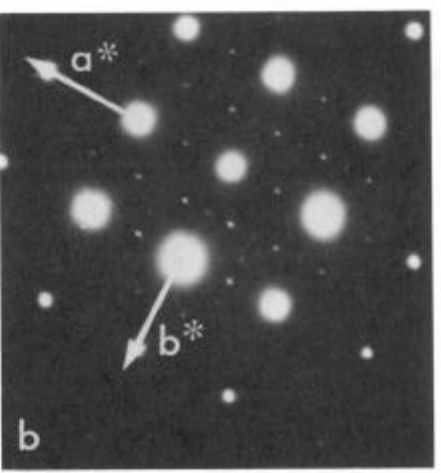


Figure 5 - Heat treated sample 8 h at 700°C, TEM examinations of the tetragonal intermetallic phase % "Ni3Nb. a) bright field - b) [001] % SAD pattern.

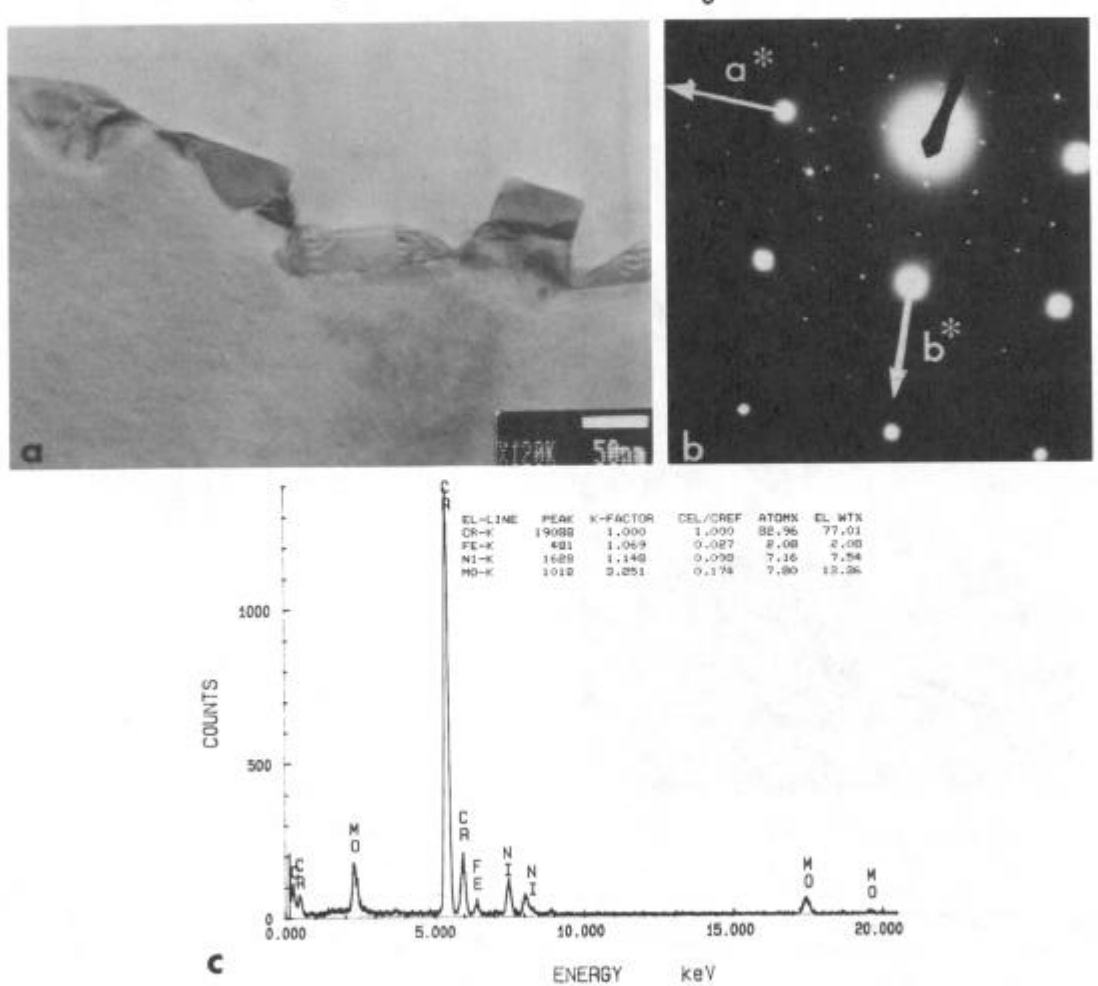
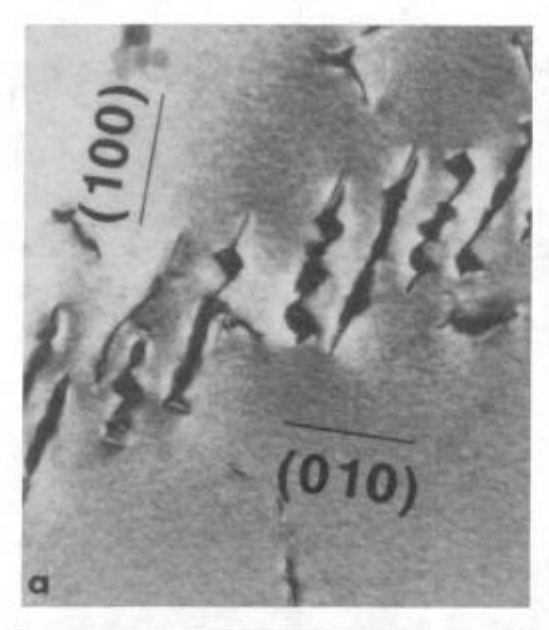
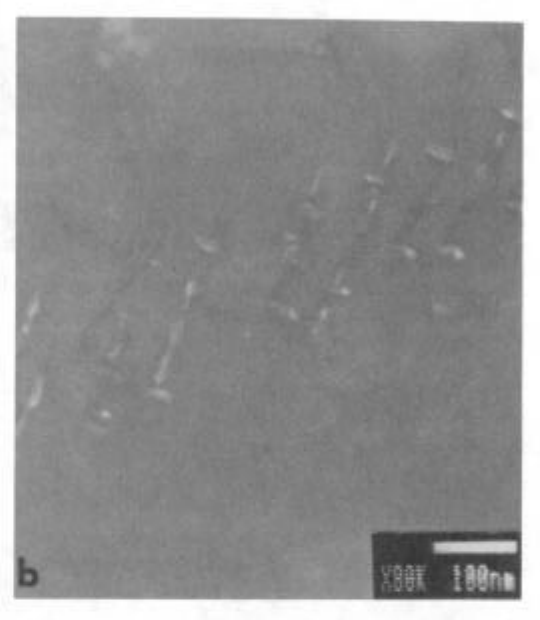


Figure 6 - Heat treated sample 8 h at 700°C, TEM examinations of intergranular M23C6 carbides. a) bright field - b) [001] γ and M23C6 SAD pattern

of M23C6 carbide -c) typical X-EDS microanalysis.

From $750\,^{\circ}\text{C}$ above, the dislocation glidings intensity decreases and 6 " particles are only segregated on matrix dislocations (Fig.7).





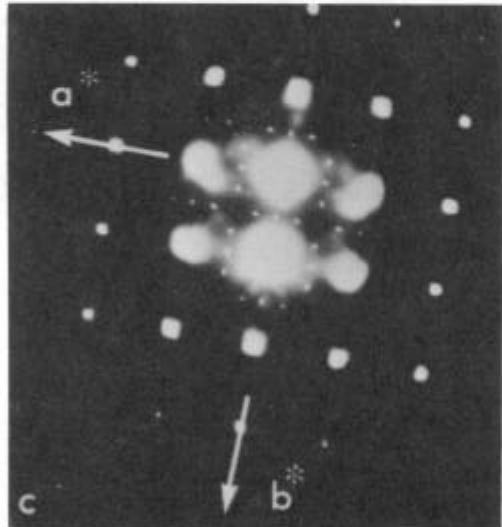


Figure 7 - Heat treated sample 8 h at 750°C,
TEM examinations of " particles.

- a) bright field -
- b) corresponding dark field -
- c) [001] Y SAD pattern used for dark field in b).

At 850°C, dislocation glidings and 8" phase have disappeared. From 800°C above, the intergranular (grain and twin boundaries) precipitates are strongly associated and X-EDS microanalysis indicates a wide range of chemical compositions from Cr rich carbides to Mo, Nb, Cr, Si rich carbides (Fig.8). At 900°C, M6C carbides coarsen and at 1000°C, all M23°C6 carbides have disappeared. Above 1000°C, M6C carbides shorten in size and their number decreases whereas small MC carbides (M = Nb, Ti, Mo) are observed at and near 8 matrix grain boundaries (Fig.9).

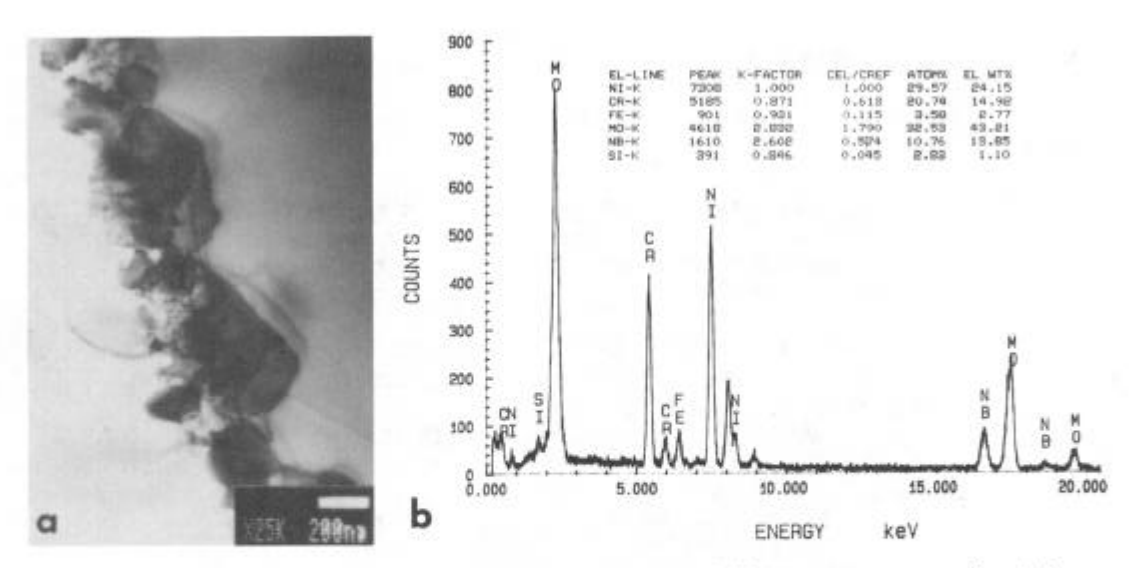
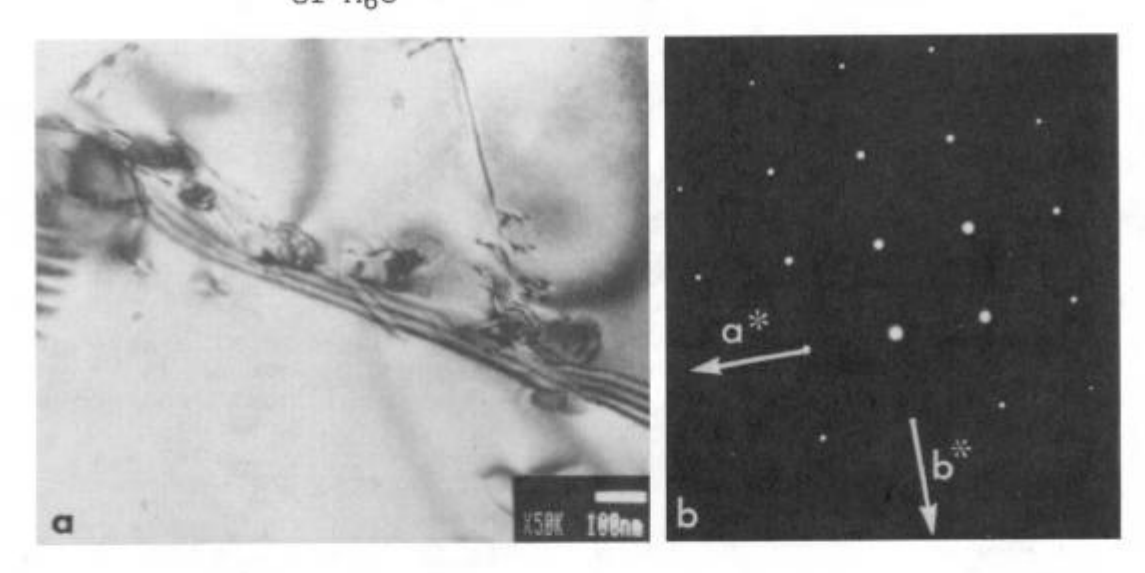


Figure 8 - Heat treated sample 8 h at $800\,^{\circ}\text{C}$, TEM examinations of intergranular carbides precipitation.
a) bright field - b) typical X-EDS microanalysis of M_6C



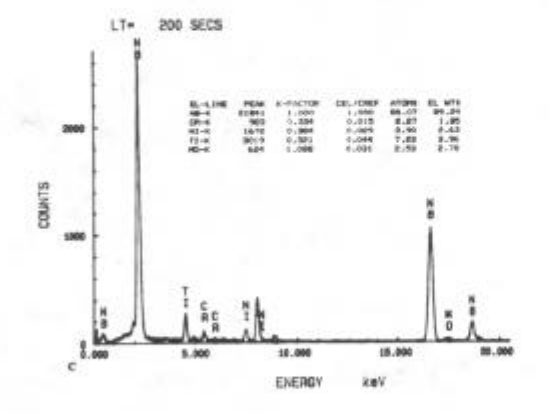


Figure 9 - Heat treated sample 8 h at 1050°C, TEM examinations of MC carbides precipitation.
a) bright field b) [001] SAD pattern c) typical X-EDS micro-analysis.

Mechanical properties in relation to structural changes

Heat treatments influence the mechanical behaviour of alloy 625 in the range of 650-950°C.

Hardness (Fig.10) and tensile strength : YS(0.2%offset), UTS $\overline{\text{(Fig.11)}}$ increase for heat treatments between 650 and 800°C, with the maximum hardening at 750°C, corresponding to three microstructural events :

- dislocation gliding of χ matrix under influence of internal stresses before and during tetragonal χ " Ni₃Nb precipitation,
- tetragonal & " Ni3Nb precipitation,
- M23C6 carbides formation at grain and twin boundaries.

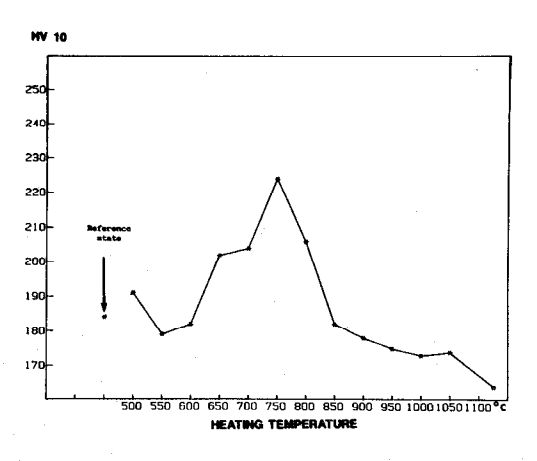


Figure 10 - Hardness curve VS heat treatments.

Figure 11 - Tensile strength curves VS heat treatments UTS

Elongation does not vary significantly (Fig.12).

500 550 600 650 700 750 800 850 900 850 1000 1050 1100 °C
HEATING TEMPERATURE

290240200160500 550 660 650 760 750 800 850 1000 1050 1100*C

HEATING TEMPERATURE

Figure 12 - Ductility curves VS heat treatments

RA EL

Figure 13 - Effect of heat treatments on CHARPY V-notch impact strength

Reduction of area (Fig.12) and CHARPY impact strength (Fig.13) are the most significant to reveal influence of heat treatments on alloy 625 mechanical properties. They are minima for heat treatments between 750 and 950°C corresponding to $M_{23}C_6$ carbides intergranular precipitation. Fracture surfaces are intergranular ductile with small dimples (Fig.14). Brittleness of grain and twin boundaries is due to intergranular precipitation of both carbides.



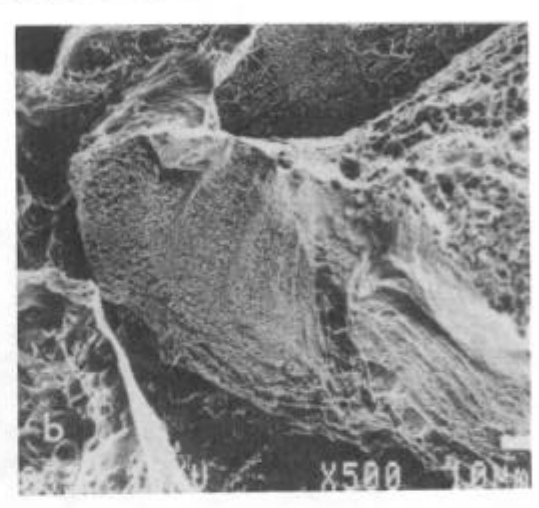


Figure 14 - Scanning electron micrographs of fracture surfaces of lowest CVN values specimens (heat treated sample 1 h at 900°C presented here).

a) general view -

b) detail of the intergranular ductile fracture.

ASTM G 28 intergranular corrosion resistance

The ASTM G 28 intergranular results are shown in figure 15.

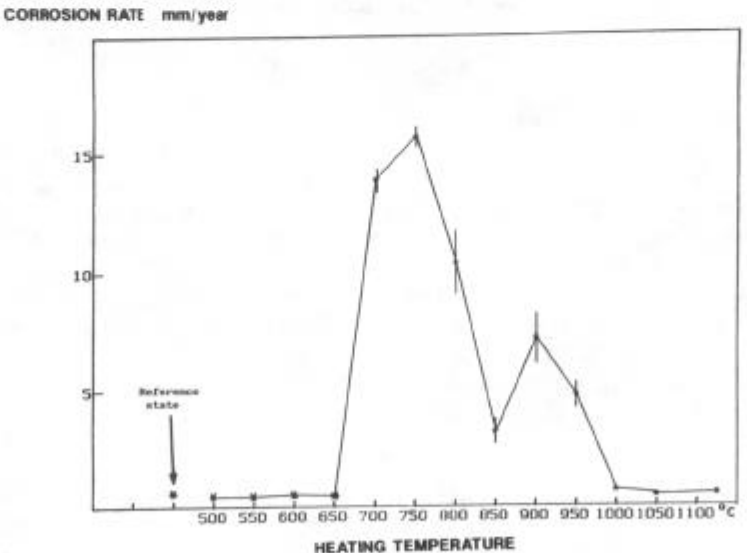
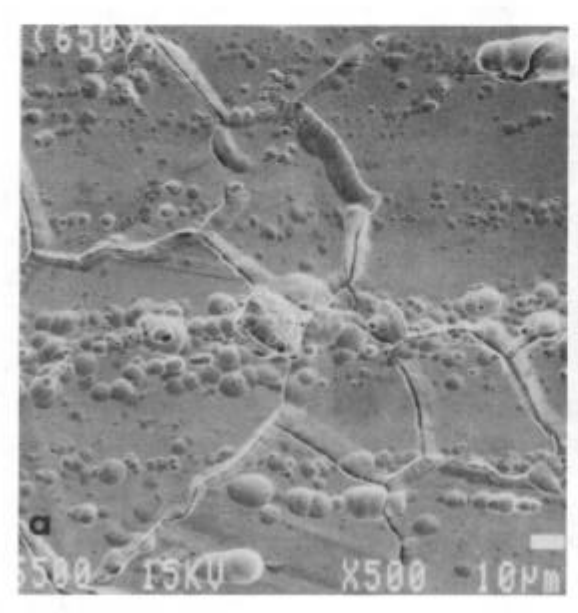


Figure 15 - Effect of heat treatments on ASTM G 28 test susceptibility.

Before 650°C, intergranular corrosion is very weak (Fig.16 a) and attack areas are localized on oxide inclusions in segregation bands. Samples heat treated between 700 and 950°C suffer considerable corrosion. In our case, it is maximum at 700 and 750°C (Fig.16 b), corresponding to existence of rich chromium carbides at grain and twin boundaries. Intergranular corrosion decreases when heat treatment temperature grows, as M23C6 carbides disappear, and then M6C.



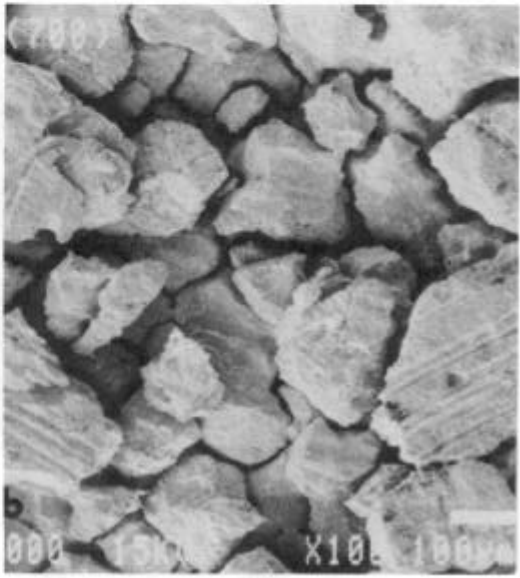


Figure 16 - Scanning electron micrographs showing corrosion attack areas after ASTM G 28 test.

- a) heat treated sample 8 h at 650°C -
- b) heat treated sample 8 h at 700°C.

Conclusion

Alloy 625 is wellknown for its good mechanical characteristics, weldability and corrosion resistance. It may be used to weld, to repair or to clad low alloy steels or HSLA steels. For post-weld heat treatments, we need to possess adequate informations on heat treatment effects on structure and properties of alloy 625. This was studied by means of optical and electron microscopy, tensile tests, CHARPY impact tests and ASTM G 28 intergranular corrosion tests. A 20 mm thick forged rod, solution treated 1 h at 1125°C and water quenched, was then heat treated at 500 to 1125°C during 8 h and air cooled. Most significant results are:

- dislocation glidings of the fcc matrix take place before and during precipitation of the intermetallic tetragonal $\uprecept{3}$ " Ni₃Nb phase, from 650°C above, due to internal stresses.
- industrial heat treatments of alloy 625 in the 650-850 $^{\circ}\text{C}$ range must be avoided because of drop of :

- * reduction of area,
- * impact strength,
- * ASTM G 28 intergranular corrosion resistance,

all resulting from $M_{23}C_6$ and M_6C rich chromium carbides precipitation at grain and twin boundaries.

Acknowledgments

The authors would like to thank greatfully Anne Poher for STEM investigations and Didier Louérat for SEM investigations.

References

- 1. "INCONEL alloy 625" HUNTINGTON Alloys Inc., Huntington, West Virginia, <u>Publication n°3700 -</u> Revised (November 1981).
- 2. P.E.MANNING et al., "Evaluation of High Performance Alloys Used in the Pulp and Paper Industry", Materials Performance, (January 1984), 19-24.
- 3. "Marine applications for INCONEL alloy 625 weld overlays", Anti-corrosion, (February 1982), 10.
- M.CONOVER, P.ELLIS and A.CURZON, "Material Selection Guidelines for Geothermal Power -An Overview", ASTM STP 717, ASTM, (1980), 24-40.
- 5. R.COX, "Refurbishing makes economic sense", Corrosion and maintenance, (April-June 1985), 97-98.
- R.M.NUGENT, "Alloy 625 Surfacing tool and die steels", Welding Journal, (june 1986), 33-39.
- 7. T.J.GLOVER, Paper n°16 presented at the 10th International Conference of the British Pump Manufacturers'Association, (Cambridge), Great-Britain 22-25 March 1987.
- 8. A.VAN BEST, Ph.DARGENT, "Electroslag cladding using nickel base alloys", <u>Metal Constructions</u>, (December 1983), 730-733.
- 9. C.E.STEVENS, R.ROSS Jr, "Production, Fabrication and Performances of Alloy 625 clad steel for agressive corrosive environments", <u>J. of Materials for energy Systems</u>, Vol.8, n°1, (June 1986), 7-11.
- 10. P.KOSHY, "Alloy 625 weld cladding of wellheads and valves: Review of dilution control techniques and weld process development", Paper presented at the 17th Offshore Technology Conference, HOUSTON, (Texas), (06-09 may 1985), 145-153.

- 11. S.C.HAYES, "Heat treatments parameters for the aging of Alloy 625", KAPL- 4143 UC-25 (DOE/TIC-4500 R69), (September 1981).
- 12. J.P.HAMMOND, "Ductility minimum and its reversal with prolonged aging in cobalt- and nickel-based superalloys", Paper presented at the ASME Winter Annual Meeting on Ductility and Toughness Considerations in elevated temperature Service" San Francisco, Californie, 10-15 December 1978, ASME (MPC 8), NY, (1978), 63-67.
- 13. K.KROMPHOLTZ, R.TIPPING and G.UHLRICH, "Investigations into the influence of the top velocity and the heat treatment on the dynamic fracture toughness of INCONEL 625", Z.Werkstofftech. 15, (1984), 199-206.